

## Characteristics and mechanism of persulfate activated by natural siderite for water disinfection

Guo-Qiang Li<sup>a,b</sup>, Chaoyi Wang<sup>a</sup>, Yingying Zhang<sup>a</sup>, Hongyou Wan<sup>a,b,\*</sup>, Ming Dou<sup>a,b</sup> and Hongbin Xu<sup>a,b</sup>

<sup>a</sup> School of Ecology and Environment, Zhengzhou University, 450001 Zhengzhou, Henan, China

<sup>b</sup> Research Centre of Engineering and Technology for Synergetic Control of Environmental Pollution and Carbon Emissions of Henan Province, 450001 Zhengzhou, China

\*Corresponding author. E-mail: hywan@zzu.edu.cn

 HW, 0000-0002-4315-3002

### ABSTRACT

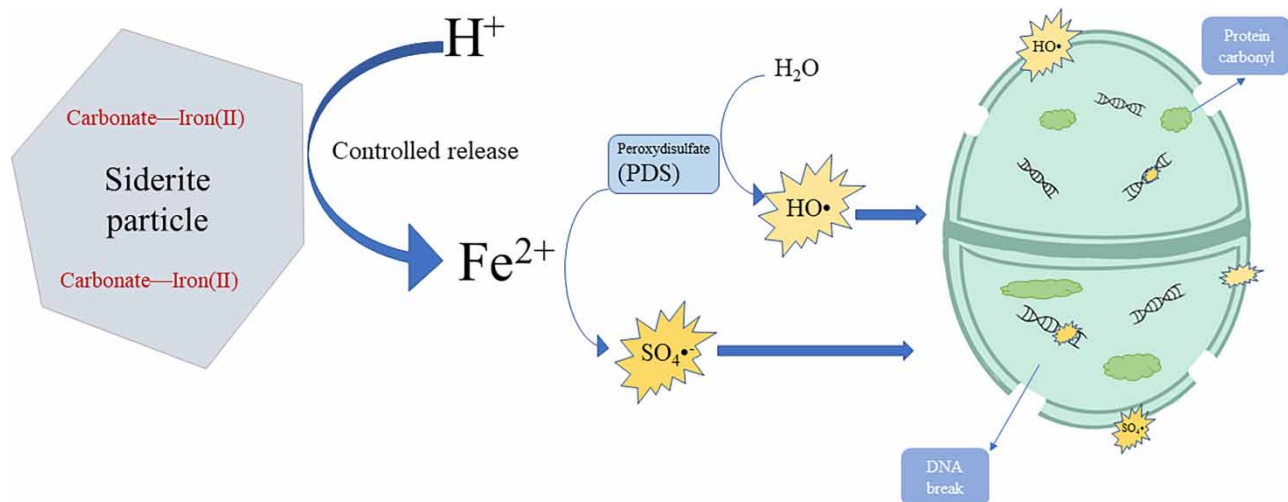
In this study, low-cost siderite was used to activate peroxydisulfate (PDS,  $S_2O_8^{2-}$ )-inactivated *Enterococcus faecalis* to study the inactivation characteristics and mechanism of siderite/PDS. The results showed that the siderite/PDS had a better inactivation effect on *Enterococcus faecalis* at pH 3. The sterilization effect increases with the increase of siderite dosage, PDS concentration and temperature. The inactivation rate is decreased with the increase of initial bacterial concentration. Inorganic ions and natural organic matter (NOM) can inhibit the inactivation effect of this technology, and the inhibition intensity is  $NOM > HCO_3^- > NO_3^-$ . The free radical quenching test shows that  $HO^\bullet$  is the main oxidizing substance in the sterilization process of siderite/PDS technology. In addition, the main disinfection mechanism is highly reactive oxygen species destroying the cell wall of bacteria and releasing organic compounds in cells. After siderite was reused for four times, simply washing siderite would recover almost 80% of the removal of *Enterococcus faecalis* in siderite/PDS, indicating that siderite has the potential of recycling.

**Key words:** disinfection, *Enterococcus faecalis*, persulfate, siderite

### HIGHLIGHTS

- *Enterococcus faecalis* (Gram-positive bacteria), a typical disinfection residue bacteria, was used as the indicator microorganism.
- The economic and efficient natural siderite was used as the activator of persulfate, and the reusability and structural stability of the recovered siderite are also analyzed.

### GRAPHICAL ABSTRACT



This is an Open Access article distributed under the terms of the Creative Commons Attribution Licence (CC BY-NC-ND 4.0), which permits copying and redistribution for non-commercial purposes with no derivatives, provided the original work is properly cited (<http://creativecommons.org/licenses/by-nc-nd/4.0/>).

## 1. INTRODUCTION

According to the data of the World Health Organization (WHO), about one-third of people's drinking water in the world is polluted by feces (World Health Organization 2016). The pathogenic microorganisms in the water are an important cause of water-borne diseases and may cause pipeline corrosion and membrane pollution, which seriously affect the health and development of humans and animals (Mcguigan *et al.* 2012; Mao *et al.* 2021). Disinfection is one of the methods to control pathogenic microorganisms in wastewater treatment plants. At present, common disinfection processes include ultraviolet disinfection, ozone disinfection, chlorination disinfection, etc. (Kong *et al.* 2021b). Nevertheless, scarcely any of the disinfection method could inactivate all microorganisms in water in full-scale applications (Proctor & Hammes 2015); there are always some microorganisms that can maintain growth ability or toxicity after disinfection, which is called disinfection residual bacteria (DRB) (Wang *et al.* 2021). DRB will not only cause membrane pollution and pipeline corrosion in the process of water treatment (Cui *et al.* 2020) but also may cause biological pollution and greatly increase the cost of water treatment (Emily *et al.* 2018; Yu *et al.* 2018). Therefore, it is necessary to improve the traditional disinfection methods to effectively control a series of risks caused by pathogenic microorganisms.

Disinfection processes could have a selection effect on Gram-positive/negative bacteria. Gram-negative bacteria have a cytoplasmic membrane, a thin peptidoglycan layer and an outer membrane containing lipopolysaccharides. However, Gram-positive bacteria have only a cytoplasmic lipid membrane, and the peptidoglycan layer is thicker than that of Gram-negative bacteria. Because of these structural differences, Gram-positive bacteria such as *Enterococcus faecalis* are usually more resistant to disinfection treatments based on radicals' oxidation than Gram-negative bacteria such as *Escherichia coli* (Rodríguez-Chueca *et al.* 2014, 2019b). Thus, they are easier to remain in the disinfection process as DRB. Bianco *et al.* mentioned that *Enterococcus faecalis* is another indicator microorganism with higher resistance than commonly used *E. coli* in advanced oxidation process (AOP) disinfection (Bianco *et al.* 2017). However, most studies used *E. coli* as a model microorganism for water disinfection, for example, Wang *et al.* used visible light to activate persulfate to completely inactivate *E. coli* without catalyst (Wang *et al.* 2019). Tong *et al.* used magnetic Fe<sub>3</sub>O<sub>4</sub> deposited flower-like MoS<sub>2</sub> nanocomposites for the Fenton-like *E. coli* disinfection (Tong *et al.* 2020). Ferreira *et al.* studied solar-activated persulfate-inactivated pathogenic microorganisms in water, and *E. coli* was also used as the indicator microorganism, which would overestimate the inactivation efficiency of AOPs (Ferreira *et al.* 2020).

In recent decades, sulfate radical (SO<sub>4</sub><sup>•-</sup>)-based AOPs (SR-AOPs) have attracted increasing interest in water treatment due to their high efficiency in degrading a wide range of recalcitrant micro-contaminants and even inactivating biohazards (Rastogi *et al.* 2009; Ismail *et al.* 2017; Lutze *et al.* 2017; Hammouda *et al.* 2018; Rodríguez-Chueca *et al.* 2018; Pan *et al.* 2021), which have potential as an alternative to traditional disinfection (Waldemer *et al.* 2007; Rodríguez-Chueca *et al.* 2016, 2017; Bianco *et al.* 2017; Marjanovic *et al.* 2018). Persulfate can generate sulfate radical under certain conditions and further react to produce hydroxyl radical (HO<sup>•</sup>) and other highly active reactive substances. Sulfate radical has a high redox potential (hydroxyl radicals: 2.7–2.8 V, sulfate radicals: 2.5–3.1 V), broad pH values ranging from 2 to 7 and a wide absorption spectrum band (SO<sub>4</sub><sup>•-</sup> absorption band is 320–520 nm and the maximum absorption peak appears around 450 nm in any solvent) (Kong *et al.* 2021a). In view of this characteristic, it can destroy the cell wall of bacteria, resulting in the rapid inactivation of bacteria. For example, Wordofa *et al.* used iron to activate persulfate, which can effectively induce the viability loss of pathogenic *E. coli* O157:H7 (Wordofa *et al.* 2017). Rodríguez-Chueca *et al.* combined Fe<sup>2+</sup> sunlight and heating to activate persulfate, which can not only effectively inactivate pathogens such as *E. coli* but also remove emerging organic micropollutants (Rodríguez-Chueca *et al.* 2019a). However, these studies are based on *E. coli* (Gram-negative bacteria) as indicator microorganisms in the actual disinfection process, and Gram-positive bacteria are more likely to remain because of their high resistance to treatment. The characteristics and mechanism of inactivation of Gram-positive bacteria by SR-AOPs need to be studied.

Heating, microwave, UV and the addition of transition metal or carbon materials can activate persulfate to produce sulfate-free radicals. Among them, the transition metals (zero valence iron, Co<sub>3</sub>O<sub>4</sub>, CuO/Fe<sub>3</sub>O<sub>4</sub>, etc.) are neither consumed nor energy consumed in the activation process (Yin *et al.* 2021). Traditional AOPs are more efficient but more expensive than other disinfection methods. Therefore, it is necessary to develop a low-cost catalyst with a wide range of sources. Fe<sup>2+</sup> has been widely studied as it is widely sourced on the earth, cheap and easy to obtain. However, as an activator, dissolved Fe<sup>2+</sup> is easy to be oxidized into ferric mud by the oxidant. Heterogeneous material to activate persulfate can continuously precipitate ferrous ions as an activator. Among them, the mineral material containing ferrous is very promising as the

source of  $\text{Fe}^{2+}$ , because the active sites on the mineral material are independent of the reduction of ferric ions, which may improve the reactivity of iron-activated persulfate (Feng *et al.* 2018). Siderite ( $\text{FeCO}_3$ ) is an iron ore with an important economic value. It is an important part of many sediments (Kholodov & Butuzova 2008) and a common product of iron material corrosion in a submerged environment. Under acidic conditions, carbonate in siderite can react with  $\text{H}^+$  to release  $\text{Fe}^{2+}$  and activate persulfate to produce  $\text{SO}_4^{\bullet-}$ . Feng *et al.* used siderite to activate persulfate to degrade phenol, which can degrade 100% phenol, and proved that siderite is mainly used as the source of ferrous ions to activate persulfate (Feng *et al.* 2018). Yan *et al.* studied the reaction mechanism of siderite-catalyzed degradation of trichloroethylene (TCE) by hydrogen peroxide and persulfate (Yan *et al.* 2015). The results showed that TCE was completely degraded in the binary catalytic system of siderite-activated  $\text{H}_2\text{O}_2$  and  $\text{S}_2\text{O}_8^{2-}$ . Li *et al.* studied the oxidation reaction of the  $\text{H}_2\text{O}_2/\text{S}_2\text{O}_8^{2-}$  system on nine representative petroleum hydrocarbons with siderite as a catalyst. The results show that the oxidation efficiency of the  $\text{H}_2\text{O}_2/\text{S}_2\text{O}_8^{2-}$  system on target petroleum hydrocarbons is more sensitive to pH than the dosage of siderite and the molar ratio of  $\text{H}_2\text{O}_2:\text{S}_2\text{O}_8^{2-}$ . These studies prove that siderite is a promising activator to persulfate. However, the disinfection efficiency and mechanism of bacteria inactivation by the siderite/sulfate process are seldom studied (Li *et al.* 2020).

Persulfate mainly includes peroxymonosulfate (PMS,  $\text{HSO}_5^-$ ) and peroxydisulfate (PDS,  $\text{S}_2\text{O}_8^{2-}$ ); they are stable in the solid state, but PDS is cheaper than PMS and the redox potential is higher. Therefore, PDS was selected as an oxidant in this experiment (Qiao *et al.* 2021). In order to determine the activity and applicability of the siderite/PDS system, the inactivation kinetics of *Enterococcus faecalis* under different initial pH, siderite dosage, PDS concentration, bacterial concentration temperature and actual water matrix were measured in this study. In addition, biomolecular analysis was used to monitor the destruction of cytoplasmic proteins and chromosomal DNA during treatment. What is more, the reusability and structural stability of the recovered siderite are also analyzed, which provides help for the development of more economical and effective disinfection methods.

## 2. MATERIALS AND METHODS

### 2.1. Experimental reagent

The materials used were siderite powder (Wuhan Iron and steel (Group) Co., Ltd), chemical scavengers: methanol,  $\text{FeSO}_4 \cdot 7\text{H}_2\text{O}$ , tert-butyl alcohol (Tianjin Kemio Chemical Reagent Co., Ltd), sodium persulfate ( $\text{Na}_2\text{S}_2\text{O}_8$ ) (Zhengzhou Penny Chemical Reagent Factory), sodium thiosulfate ( $\text{Na}_2\text{S}_2\text{O}_3 \cdot 5\text{H}_2\text{O}$ ) (Tianjin Kemio Chemical Reagent Co., Ltd) and sodium chloride (NaCl) (Tianjin Kemio Chemical Reagent Co., Ltd). The scale of this test is a small-scale laboratory test. The whole reaction process was carried out in a 100 mL beaker. The reagents purchased in this test are analytically pure without further purification. All solutions are prepared by ultrapure water (18.2  $\Omega$  cm) in heal force pure water machine.

### 2.2. Experimental instrument

XPS was used to characterize the valence state of elements on the surface of the material. SEM was used to observe the morphological characteristics of the material. In order to further prove the inactivation path of bacteria and judge whether the cell membrane is damaged by free radicals, the absorbance was measured at 280 and 260 nm by UV-Vis spectrophotometer. The extracellular protein and DNA of indicator microorganisms were determined.

### 2.3. Experimental process of sterilization

**Bacterial culture:** the inoculation steps for *Enterococcus faecalis* are as follows: 200  $\mu\text{L}$  of bacterial suspension in 100 mL liquid culture medium was taken, was then put into the shaking table, the parameters were set to 37  $^\circ\text{C}$  in 150 rpm, culture was incubated for 16–18 h, and then 2 mL of bacterial solution was taken and centrifuged in 5,000 rpm high-speed centrifuge for 5 min; after centrifugation, the working solution was used for cleaning to remove nutrients and bacterial residues in the bacterial solution, and the washing steps were repeated three times before use.

**Disinfection test:** in this test, siderite was selected as an activator, sodium persulfate as an oxidant and *Enterococcus faecalis* as indicator microorganisms. The specific operation steps of the disinfection test are as follows: 100 mL of ultrapure water was taken, 5 mM anhydrous sodium sulfate was added as the working solution, the working solutions was put into the beaker, the beaker was placed on the magnetic stirrer, a certain concentration (about  $10^6$  cfu/mL of *Enterococcus faecalis*) of the freshly cultured bacterial solution was added to the working solution as the initial bacterial concentration, the pH of the solution was adjusted with 0.1 M  $\text{H}_2\text{SO}_4$  and 0.1 M NaOH, a certain concentration of oxidant was added, and then the activator to trigger the reaction and start timing was quickly added. One milliliter of the sample was taken in a 2 mL centrifuge

tube at regular intervals, and a small amount of sodium thiosulfate was added into the centrifuge tube in advance to terminate the reaction. After gradient dilution of the sample with 9% sodium chloride solution, 100  $\mu\text{L}$  of liquid was taken into a disposable Petri dish, it was evenly spread with a coating rod, it was then inverted and incubated in a 37 °C constant temperature incubator for 18 h for plate counting. Each group was repeated three times.

The logarithmic inactivation rate of *Enterococcus faecalis* can indirectly reflect the stability and reusability of siderite. After each test, the supernatant was poured out, the siderite at the bottom of the beaker was left, the same concentration of *Enterococcus faecalis* was added and the next round of reaction was started by adding PDS. The sterilization test was repeated four times, and the siderite for the fifth sterilization test was washed and dried.

#### 2.4. Determination of $\text{Fe}^{2+}$ concentration

In order to determine the effect of effective ferrous ion in the reaction system on the sterilization effect, ferrous ion was determined and analyzed by 1,10-phenanthroline ultraviolet spectrophotometry. The principle is that  $\text{Fe}^{2+}$  and o-phenanthroline form a very stable orange-red complex at pH 2–9. The specific operation steps are as follows: 3 mL of sample solution was taken, after that 0.2 mL (1 + 4) sulfuric acid, 0.4 mL of 2 M ammonium fluoride, 0.4 mL of 1,10-phenanthroline solution, 0.6 mL of 3 M ammonium acetate buffer solution and 0.4 mL of ultrapure water were successively added, and each reagent was shaken and mixed by hand, which was allowed to develop color for 10 min. The absorbance was measured with a UV-Vis spectrophotometer at 510 nm, and then the  $\text{Fe}^{2+}$  content according to Lambert Beer's Law was calculated.

#### 2.5. Determination of bacterial concentration

In this experiment, clear bacterial colonies are counted by the standard plate counting method, and the colonies on the Petri dish are effectively detected. The measurement range is 1–300 cfu. cfu/mL is used to express the bacterial survival density, which is the coating plate method in this test. The detection limit (DL) is 10 cfu/mL. In this test, the inactivation effect of each disinfection technology is characterized by a logarithmic inactivation rate as follows:

$$\lg\left(\frac{N_0}{N_t}\right) \quad (1)$$

$N_0$  represents the bacterial concentration before inactivation, cfu/mL;

$N_t$  refers to the bacterial concentration at  $t$  min of inactivation, cfu/mL;

$t$  represents inactivation time, min.

The linear relationship between logarithmic inactivation ( $N_0/N_t$ ) and reaction time was used to describe the inactivation of siderite/PDS to *Enterococcus faecalis*. The deactivation rate constant based on time is calculated as follows:

$$k = \frac{\lg\left(\frac{N_0}{N_t}\right)}{t} \quad (2)$$

$N_0$  represents the bacterial concentration before inactivation, cfu/mL;

$N_t$  refers to the bacterial concentration at  $t$  min of inactivation, cfu/mL;

$t$  represents inactivation time, min.

#### 2.6. Inactivation mechanism analysis

In order to further elucidate the disinfection mechanism in siderite/PDS, the extracellular protein and DNA of indicator microorganisms were determined. The specific operation steps are as follows: 1 mL of bacterial suspension was added to the reaction system. After the reaction, 0.1 M sodium thiosulfate was added and mixed well. After 3 min, it was centrifuged in a high-speed centrifuge at 10,000 rpm for 15 min. The supernatant was taken and the absorbance was measured at 280 and 260 nm with a UV-Vis spectrophotometer.

### 3. RESULTS AND DISCUSSION

#### 3.1. Characterization of siderite

The SEM of siderite (Figure S1) reveals that the siderite powder is in irregular shape, with a particle size of about 10–30  $\mu\text{m}$  and many mechanical cracks on the surface. Figure S2 shows the surface element analysis of siderite before and after the reaction by XPS. Among them, at 0 min, the proportions of main elements C, O and Fe on the surface of siderite are 10.47, 77.06 and 12.46%, respectively. At 60 min, the proportions of C, O and Fe were 16.93, 74.95 and 8.12, respectively. Then, the peak splitting treatment of iron element with XPS peak fit software shows that the iron element on the surface of siderite at 0 and 60 min contains 50.39 and 54.14% Fe (II), which can prove its great potential of catalyzing PDS to produce highly reactive substances.

#### 3.2. Reactivity of different activators

Figure 1(a) shows the inactivation effect of siderite alone and PDS alone on *Enterococcus faecalis* within 60 min. Under the same conditions, siderite alone did not inactivate *Enterococcus faecalis*, while PDS alone could inactivate 1.45 log of *Enterococcus faecalis* within 60 min. In siderite/PDS, *Enterococcus faecalis* can be completely inactivated within 60 min, and the inactivation rate is 0.087 log/min.

Figure 1(b) shows the inactivation effect of siderite/PDS and  $\text{Fe}^{2+}$ /PDS on *Enterococcus faecalis* under the same conditions. Both systems can completely inactivate *Enterococcus faecalis*. However, it only takes 60 min for siderite/PDS to completely inactivate *Enterococcus faecalis*, whereas  $\text{Fe}^{2+}$ /PDS takes 180 min. The inactivation rate of siderite/PDS is almost the same at each time interval of 15 min. However, the inactivation rate of fecal *Enterococcus* by  $\text{Fe}^{2+}$ /PDS was 0.071 log/min in the first 30 min, within 30–180 min; the inactivation rates were 0.017, 0.024, 0.005 and 0.053 log/min.  $\text{Fe}^{2+}$ /PDS is faster in the first 30 min, and then the inactivation rate becomes slow. This may be due to the fact that dissolved  $\text{Fe}^{2+}$  is easy to be oxidized into ferric precipitation and cannot continue to activate oxidants to produce free radicals (Xu & Li 2010). The reaction rate of  $\text{Fe}^{2+}$ /PDS increased after 120 min. This may be due to the fact that  $\text{Fe}^{3+}$  is easy to form coagulation precipitation, thus adsorbing and removing some bacteria.

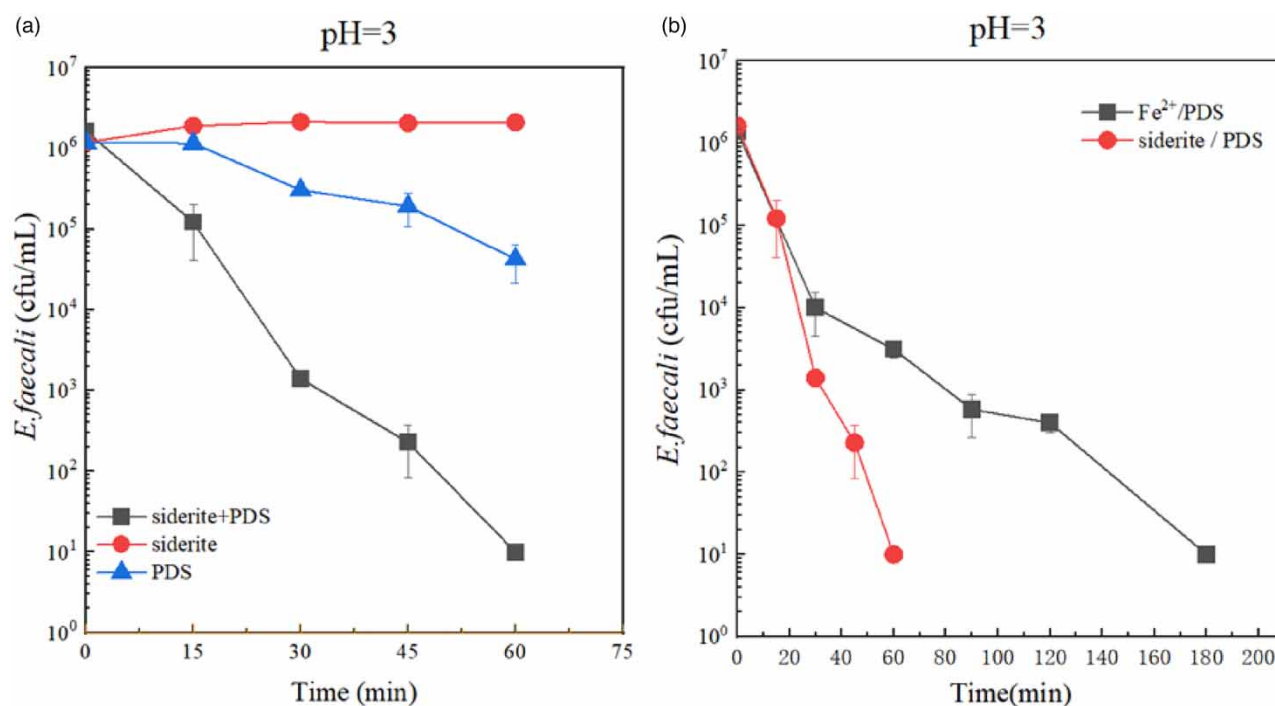


**Figure 1** | Inactivated *Enterococcus faecalis* by (a) persulfate or siderite alone and siderite/PDS technology and (b)  $\text{Fe}^{2+}$  and siderite-activated persulfates. Conditions: [PDS] = 5 mM, [siderite] = 0.5 g/L, [ $\text{Fe}^{2+}$ ] = 0.2 mM, initial pH = 3 and initial bacterial concentration =  $10^6$  cfu/mL.

### 3.3. Effect of experimental parameters

In order to determine the parameters affecting the inactivation characteristics of *Enterococcus faecalis* by siderite/PDS, the effects of pH, siderite dosage, PDS concentration, bacterial concentration and temperature were studied.

Figure 2(a) shows the effect of pH on the characteristics of siderite/PDS to inactivate *Enterococcus faecalis*. In the absence of inactivators, *Enterococcus faecalis* at different pH conditions did not significantly inactivate within 60 min. It showed that pH had no significant effect on cell viability (Figure S3). It can be seen that under the acidic condition of pH 3, siderite/PDS has a good inactivation effect on *Enterococcus faecalis*. *Enterococcus faecalis* can be completely inactivated within 60 min, and the inactivation rate is 0.087 log/min. However, with the increase in pH, the inactivation ability of the system decreased gradually. At pH 5, *Enterococcus faecalis* was inactivated by 1.04 log within 60 min, and the inactivation rate decreased to 0.017 log/min. This weak inactivation under weak acid conditions indicates that pH has a great influence. When the pH increased to 7 and 9, siderite/PDS technology has almost no inactivation ability to *Enterococcus faecalis*. It is mainly due to the low efficiency of siderite in releasing  $\text{Fe}^{2+}$  under high pH conditions, some  $\text{Fe}^{2+}$  will be converted into  $\text{Fe}^{3+}$ , which cannot catalyze PDS. The low reactivity of siderite under weak acid conditions is also reported by Huang *et al.* (2013) and Yan *et al.* (2015).

Figure 2(b) shows that the inactivation rates of *Enterococcus faecalis* increase with the dosage of siderite, which increases from 0.1 to 0.75 g/L. Comparing the reaction rate of the first 45 min, the reaction rates are 0.062, 0.07, 0.086 and 0.093 log/min in turn. However, when siderite was added to 1.0 g/L, the reaction was inhibited, only 2.85 log *Enterococcus faecalis* was inactivated in 60 min, and the reaction rate slowed down from 0.087 to 0.047 log/min. This may be because the excessive dosage of siderite leads to the release of too much  $\text{Fe}^{2+}$  in the system. Excessive  $\text{Fe}^{2+}$  consumes the free radicals, reducing the oxidation capacity of the system.

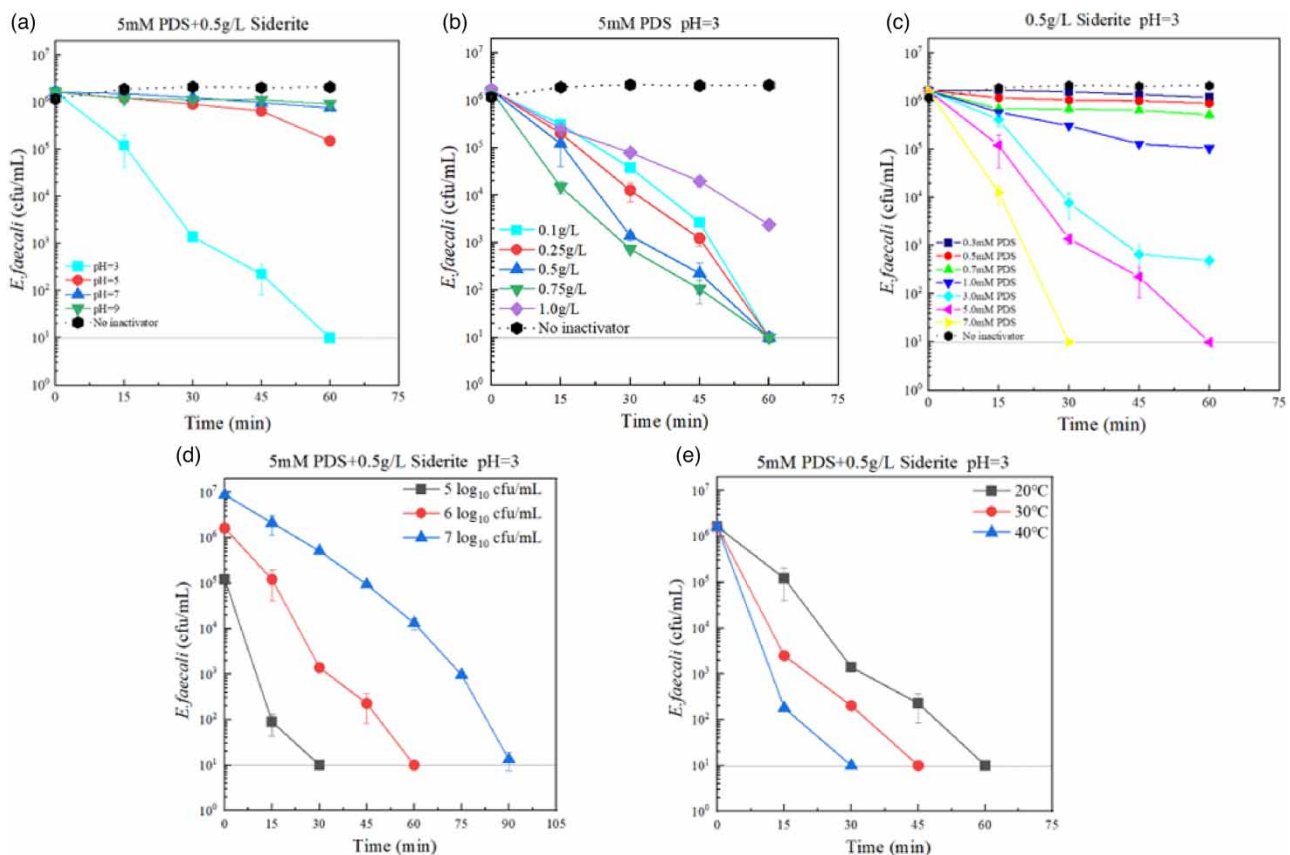


**Figure 2** | The effects of (a) initial pH, (b) siderite dosage, (c) PDS concentration, (d) bacterial concentration, and (e) temperature on the characteristics of inactivation of *Enterococcus faecalis* by siderite/PDS. Conditions: initial bacterial concentration =  $10^6$  cfu/mL.

As shown in Figure 2(c), the inactivation effect of siderite/PDS on *Enterococcus faecalis* increases with the increase of PDS concentration. When the concentration of PDS was less than 1 mM, only 1.2 log of *Enterococcus faecalis* was inactivated. When the concentration of PDS is greater than 1 mM, the sterilization effect increases with the increase of PDS concentration. Siderite/PDS inactivates 1.2 log *Enterococcus faecalis* in 60 min at 1 mM PDS to 30 min at 7 mM PDS, and the inactivation rate increases from 0.02 to 0.174 log/min.

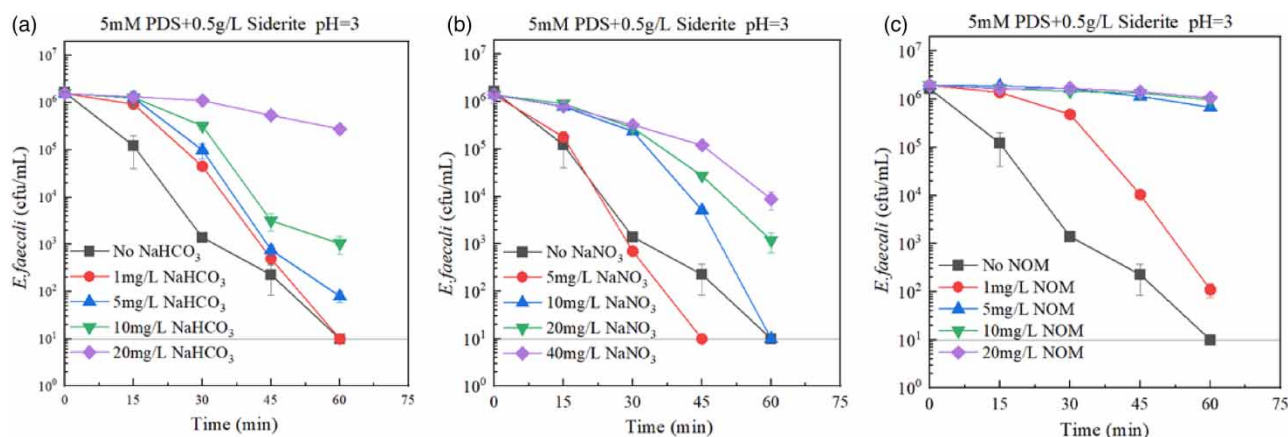
Figure 2(d) shows the effect of initial bacterial concentration on the characteristics of siderite/PDS for inactivating *Enterococcus faecalis*. It can be clearly seen that siderite/PDS can completely inactivate *Enterococcus faecalis* at three initial bacterial concentrations. However, the inactivation time is prolonged with the increase of initial bacterial concentration. For every 1 more log of *Enterococcus faecalis*, the time to complete inactivation increased by 30 min. The inactivation rates were 0.136, 0.087 and 0.065 log/min for 5, 6 and 7 log initial bacterial concentrations, respectively. Therefore, the inactivation rate of siderite/PDS for *Enterococcus faecalis* is decreased with the increase of initial bacterial concentration.

Figure 2(e) shows the effect of temperature on the characteristics of siderite/PDS for inactivating *Enterococcus faecalis*. It can be seen that as the temperature increases from 20 to 40 °C, the time for the complete inactivation of *Enterococcus faecalis* decreases from 60 to 30 min, with the inactivation rate increasing from 0.087 to 0.167 log/min, an increase of 1.9 times. This may be due to the increase of system temperature that will accelerate the thermal movement and reaction between molecules in the system. Another possibility is that heating activates PDS and produces more  $\text{SO}_4^{\bullet-}$  (Ji *et al.* 2015), improving the disinfection ability of the system. At the same time, according to this trend, it can also be inferred that the process of siderite-activating PDS is an endothermic reaction (Feng *et al.* 2016).

### 3.4. Influence of inorganic ions and natural organic matters

Natural water contains a large number of inorganic ions and natural organic substances, which serve as radicals' consumer (Michael-Kordatou *et al.* 2015; Wu *et al.* 2015). It is very necessary to study the influence of  $\text{HCO}_3^-$ ,  $\text{NO}_3^-$  inorganic ions and humic acid (the representative of natural organic substances) on the characteristics of siderite/PDS for inactivating *Enterococcus faecalis*. Figure 3 shows the effects of  $\text{HCO}_3^-$ ,  $\text{NO}_3^-$  and natural organic matter (NOM). Figure 3(a) shows that the inactivation of *Enterococcus faecalis* decreases with the increase of  $\text{HCO}_3^-$  concentration. When 20 mg/L  $\text{NaHCO}_3$  was added, the inactivation rate slowed down from 0.087 log/min in the control group to 0.012 log/min, that is, the reaction rate was inhibited by 86.2%. Wu *et al.* suggested that bicarbonate could form complexes on the catalyst surface and even quench the  $\text{SO}_4^{\bullet-}$  to generate the  $\text{CO}_3^{\bullet-}$ . The great consumption of  $\text{SO}_4^{\bullet-}$  and the relatively lower reactivity of  $\text{CO}_3^{\bullet-}$  (2.09 eV) than  $\text{SO}_4^{\bullet-}$  (2.5-3.1 eV (Lei *et al.* 2010)) would have a detrimental effect on the siderite/PDS system, thus greatly inhibiting *Enterococcus faecalis* inactivation (Wu *et al.* 2015).

A low concentration of  $\text{NO}_3^-$  improves the inactivation of *Enterococcus faecalis* in this study (Figure 3(b)). When the system contained 5 mg/L  $\text{NaNO}_3$ , the complete inactivation time of *Enterococcus faecalis* was shortened by 15 min. This may be due to the inactivation of bacteria caused by the high oxidation of  $\text{NO}_3^-$  under acidic conditions, which increases the inactivation



**Figure 3** | The effects of (a)  $\text{HCO}_3^-$ , (b)  $\text{NO}_3^-$ , and (c) NOM on the characteristics of siderite/PDS inactivation of *Enterococcus faecalis*. Conditions: [PDS] = 5 mM, [siderite] = 0.5 g/L, initial pH = 3, initial bacterial concentration =  $10^6$  cfu/mL and reaction time = 60 min.

rate (Rincon & Pulgarin 2004). However, when the concentration of  $\text{NaNO}_3$  is greater than 10 mg/L, the inhibitory effect increases with the increase of concentration. When 20 mg/L  $\text{NaNO}_3$  was added, siderite/PDS technology inactivated 2.88 log *Enterococcus faecalis*, and the inactivation rate was inhibited by 44.8%.  $\text{NO}_3^-$  may be adsorbed to the surface of the activator to reduce its catalytic activity and may react with free radicals to reduce the sterilization capacity of the system (Alrousan *et al.* 2009; Ma *et al.* 2018).

The content of NOM in water is about 10 mg/L; NOM is usually present in the aquatic environment, which can act as a radical scavenger via competing for  $\text{SO}_4^{\bullet-}$  and  $\text{HO}^\bullet$  (Matilainen *et al.* 2004). From Figure 3(c), it can be seen that when 1 mg/L NOM is added, it inhibits the sterilization ability of siderite/PDS technology, with an inhibition of 0.97 log in 60 min. When the concentration of NOM continues to increase to 5 mg/L, the reaction rate is inhibited by 90.8% and siderite/PDS technology can basically be regarded as having no disinfection capacity. The addition of NOM greatly inhibited the inactivation rate. This may be because NOM contains more phenolic hydroxyl and carboxyl groups, which can be adsorbed on the surface of the catalyst and block the reaction site (Michael-Kordatou *et al.* 2015).

According to Figure 3,  $\text{HCO}_3^-$ ,  $\text{NO}_3^-$  and NOM have a certain degree of inhibitory effect on siderite/PDS technology inactivation of *Enterococcus faecalis*, and the inhibition intensity is  $\text{NOM} > \text{HCO}_3^- > \text{NO}_3^-$ .

### 3.5. The mechanism of siderite/PDS-inactivating *Enterococcus faecalis*

In order to verify the contribution of  $\text{SO}_4^{\bullet-}$  and  $\text{HO}^\bullet$  in siderite/PDS, tert-butanol (TBA) and methanol were selected as free radical scavengers in this experiment. Methanol was used to scavenge  $\text{SO}_4^{\bullet-}$  and  $\text{HO}^\bullet$ . While TBA was used to scavenge  $\text{HO}^\bullet$  ( $k = 3.8\text{--}7.6 \times 10^8 \text{ M}^{-1}\cdot\text{s}^{-1}$ ) (Buxton *et al.* 1988), due to its reaction rate with  $\text{SO}_4^{\bullet-}$  being slow ( $k = 4.0\text{--}9.1 \times 10^5 \text{ M}^{-1}\cdot\text{s}^{-1}$ ) (Chawla & Fessenden 1975). And these chemical scavengers will not be toxic to *Enterococcus faecalis* (Xia *et al.* 2017).

The experimental results are shown in Figure 4. After adding a free radical scavenger, the disinfection effect of the system is inhibited, indicating that the disinfection ability of the system is related to the content of free radicals. When 5 mM methanol was added, siderite/PDS inactivated 0.77 log *Enterococcus faecalis* within 60 min, the inactivation rate was 0.013 log/min and the disinfection ability was inhibited by 85.1%. When 5 mM TBA was added, siderite/PDS inactivated 1.53 log *Enterococcus faecalis* within 60 min, the inactivation rate was 0.025 log/min and the disinfection ability was inhibited by 71.3%. That is, the removal of  $\text{SO}_4^{\bullet-}$  and  $\text{HO}^\bullet$  inhibited the disinfection capacity of the system by 13.8 and 71.3%, respectively, which shows that  $\text{HO}^\bullet$  contributes greatly to the sterilization process of siderite/PDS technology. However, since inhibition is not complete, there is a part of the disinfection that is not due to the action of any of the radicals studied, which could indicate the combination with non-radical pathways (Guerra-Rodriguez *et al.* 2022).

Figure 5 shows the results of extracellular protein and DNA before and after the siderite/PDS inactivation of *Enterococcus faecalis*. It can be seen from the figure that in siderite/PDS, the levels of extracellular protein and DNA increased rapidly after the inactivation of *Enterococcus faecalis*.

The results showed that high reactive oxygen species could destroy the cell wall of *Enterococcus faecalis*, releasing organic macromolecules in the cells (Sun *et al.* 2014), and then lead to the inactivation of *Enterococcus faecalis* cells. When the inactivation reaction continued for 300 min, the protein and DNA decreased to 26.27 and 22.12  $\mu\text{g/mL}$ , respectively, which may be because the extracellular protein and DNA are organic macromolecules, while the high reactive oxygen species of  $\text{SO}_4^{\bullet-}$  and  $\text{HO}^\bullet$  in the system will degrade or even mineralize the organic matter, resulting in a downward trend in the content of extracellular protein and DNA.

### 3.6. Reuse analysis of siderite

The recycling of the activator is a major factor to be considered in reducing the operation cost of the process in practical application.

Figure 6 shows the reused siderite active PDS for inactivating *Enterococcus faecalis*. It can be seen that in the first four tests, siderite/PDS inactivated 3.07, 2.71, 2.3 and 1.98 log *Enterococcus faecalis*, respectively. With the increase of siderite reuse times, the inactivation ability gradually decreases. This may be related to some active sites on the surface of siderite adsorbing the oxidation products of *Enterococcus faecalis* or  $\text{Fe}^{2+}$  on its own surface is oxidized. After washing and drying the siderite, it was found that 2.38 log *Enterococcus faecalis* removal was obtained, and the inactivation efficiency returned to 78% of the initial operation level. This may be due to the removal of bacterial residues on the surface of siderite after water washing, and the characteristic peak of its organic functional groups was greatly weakened (Xia *et al.* 2017).



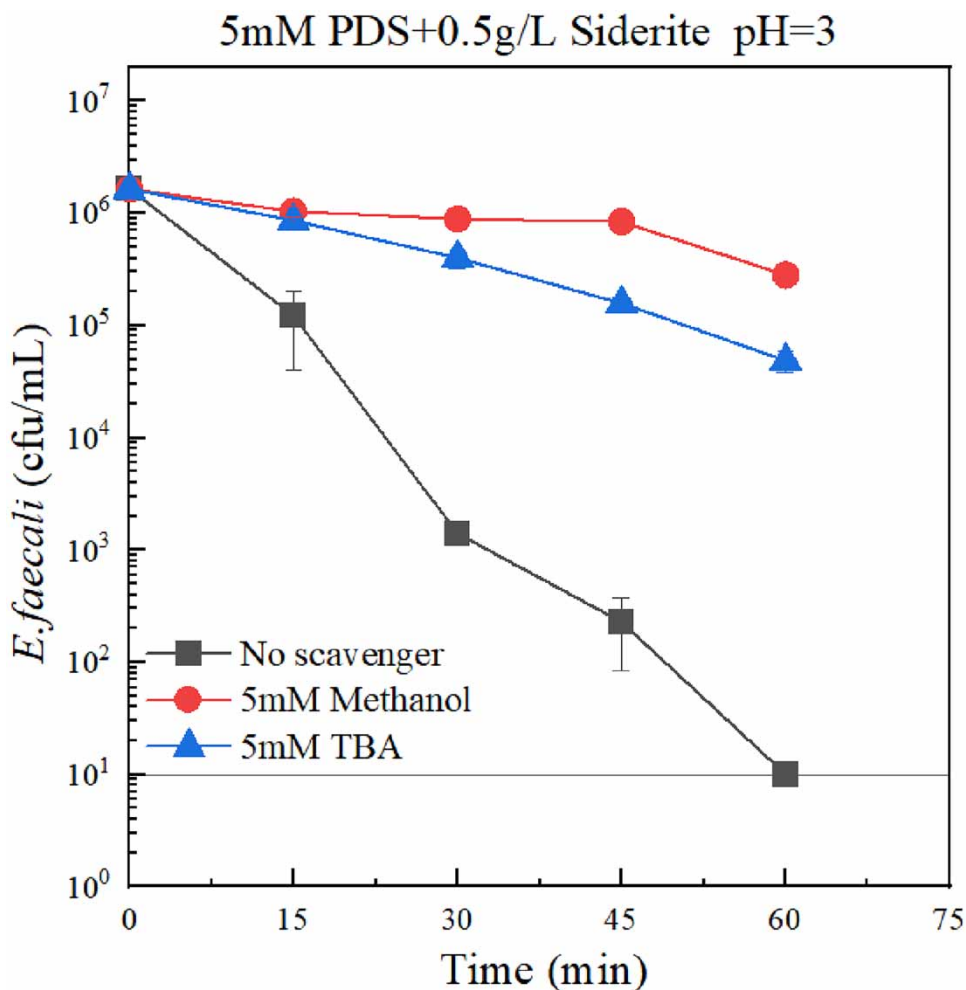


**Figure 4** | The quenching effect of methanol and TBA on siderite/PDS inactivation of *Enterococcus faecalis*. Conditions: [PDS] = 5 mM, [siderite] = 0.5 g/L, initial pH = 3, initial bacterial concentration = 10<sup>6</sup> cfu/mL and reaction time = 60 min.

### 3.7. Disinfection characteristics of siderite/PDS in actual water matrix

The actual water (AW) used in this test is the effluent from the V-shaped filter of an urban domestic sewage treatment plant, with a pH value of about 7.40. Before the disinfection test, the water sample is filtered through a 0.45  $\mu$ m filter membrane to remove particulate matter and most microorganisms. *Enterococcus faecalis* in the experiment was cultured and added in the later stage, and the initial concentration of bacteria added was not properly reduced but kept consistent with the initial concentration of bacteria in self-distribution water (SDW). Its purpose was mainly to study the disinfection performance of siderite/PDS technology rather than engineering application. Figure S4 shows the inactivation effect of siderite/PDS technology on *Enterococcus faecalis* in the effluent matrix of the filter. It can be seen from the figure that siderite/PDS technology can only inactivate 1.27 log of *Enterococcus faecalis* in the effluent matrix of a V-shaped filter for 60 min, and the inactivation rate is 0.021 log/min. It can inactivate 5 log of *Enterococcus faecalis* in self-distribution water, and the inactivation rate is 0.086 log/min. This is mainly because there are many kinds of ions in the actual water matrix. Some ions have the characteristics of scavenging free radicals, thus reducing the oxidation capacity of the system and deteriorating the disinfection effect. The specific influencing factors need to be further explored.

## 4. CONCLUSIONS

The characteristics and mechanism of siderite-activated persulfate for inactivating *Enterococcus faecalis* were determined in this study. The main conclusions are as follows: siderite/PDS is able to effectively inactivate *Enterococcus faecalis* at 5 mM

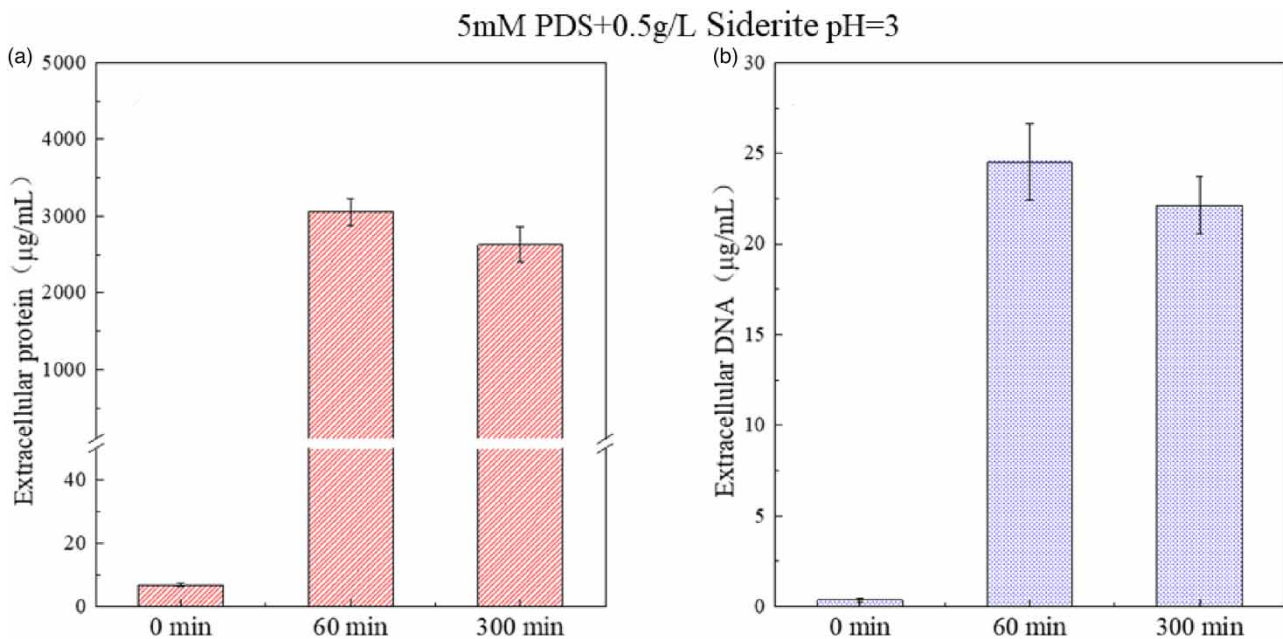


**Figure 5** | The determination of (a) extracellular proteins and (b) DNA of *Enterococcus faecalis* at 0, 60 and 300 min inactivation by the siderite/PDS technique. Conditions: [PDS] = 5 mM, [siderite] = 0.5 g/L, initial pH = 3 and initial bacterial concentration =  $10^6$  cfu/mL.

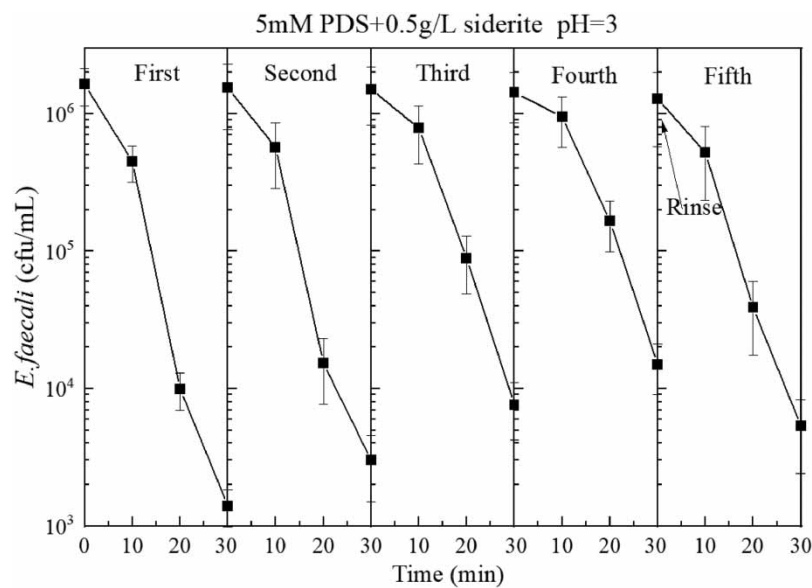


**Figure 6** | The effect of siderite reuse on the characteristics of siderite/PDS technology in inactivating *Enterococcus faecalis*. Conditions: [PDS] = 5 mM, [siderite] = 0.5 g/L, initial pH = 3, initial bacterial concentration =  $10^6$  cfu/mL and reaction time = 60 min.

PDS and 0.5 g/L siderite in 60 min. Siderite/PDS has a better inactivation effect on *Enterococcus faecalis* when the pH value of the environment is 3. The increase of siderite dosage and PDS concentration in a certain range can promote the inactivation effect of siderite/PDS technology on *Enterococcus faecalis*. Within 20–40 °C, the higher the temperature, the higher it elevates the inactivation rate.  $\text{HCO}_3^-$ ,  $\text{NO}_3^-$  inorganic anions and NOM have a certain degree of inhibition on siderite/PDS in disinfection, and the inhibition intensity is  $\text{NOM} > \text{HCO}_3^- > \text{NO}_3^-$ . After siderite was reused four times, simply washing siderite would recover almost 80% of the removal of *Enterococcus faecalis* in siderite/PDS. Through the free radical

quenching test, it is found that HO<sup>•</sup> is the main oxidizing substance in the sterilization process of siderite/PDS. In addition, the mechanism of *Enterococcus faecalis* inactivated by siderite/PDS technology was determined by measuring the extracellular protein and DNA. High reactive oxygen species destroyed the cell wall of *Enterococcus faecalis*, and the organic macromolecules in the cells flowed out, resulting in the inactivation of *Enterococcus faecalis*. However, the inactivation of microorganisms of siderite/PDS needs to be further studied in actual water in order to provide optimal parameters for engineering application.

## ACKNOWLEDGEMENT

This work was supported by the Research Institute for Environmental Innovation (Suzhou), Tsinghua (No. 00010272), the Key R&D and Promotion Project of Henan Province (No. 222102320094) and the Postdoctoral Research Grant in Henan Province (No. 20190212).

## DATA AVAILABILITY STATEMENT

All relevant data are included in the paper or its Supplementary Information.

## CONFLICT OF INTEREST

The authors declare there is no conflict.

## REFERENCES

- Alrousan, D. M. A., Dunlop, P. S. M., McMurray, T. A. & Byrne, J. A. 2009 Photocatalytic inactivation of *E. coli* in surface water using immobilised nanoparticle TiO<sub>2</sub> films. *Water Research* **43**, 47–54.
- Bianco, A., Polo-Lopez, M. I., Fernandez-Ibanez, P., Brigante, M. & Mailhot, G. 2017 Disinfection of water inoculated with *Enterococcus faecalis* using solar/Fe(III)EDDS-H<sub>2</sub>O<sub>2</sub> or S<sub>2</sub>O<sub>8</sub><sup>2-</sup> process. *Water Research* **118**, 249–260.
- Buxton, G. V., Greenstock, C. L., Helman, W. P. & Ross, A. B. 1988 Critical review of rate constants for reactions of hydrated electrons. *Journal of Physical and Chemical Reference Data* **17** (2), 513–886.
- Chawla, O. P. & Fessenden, R. W. 1975 Electron spin resonance and pulse radiolysis studies of some reactions of peroxysulfate (SO<sub>4</sub><sup>•-</sup>). *The Journal of Physical Chemistry* **79**, 2693–2700.
- Cui, Q., Liu, H., Yang, H. W., Lu, Y., Chen, Z. & Hu, H. Y. 2020 Bacterial removal performance and community changes during advanced treatment process: a case study at a full-scale water reclamation plant. *The Science of the Total Environment* **705**, 135811.
- Emily, G., Jean, M. L., Jolene, B., David, E., Edwards, M. A. & Amy, P. 2018 Microbial ecology and water chemistry impact regrowth of opportunistic pathogens in full-scale reclaimed water distribution systems. *Environmental Science and Technology* **52**, 9056–9068.
- Feng, Y., Deli, W., Yun, D., Tong, Z. & Kaimin, S. 2016 Sulfate radical-mediated degradation of sulfadiazine by CuFeO<sub>2</sub> rhombohedral crystal-catalyzed peroxymonosulfate: synergistic effects and mechanisms. *Environmental Science & Technology* **50**, 3319–3327.
- Feng, Y., Wu, D., Li, H., Bai, J., Hu, Y., Liao, C., Li, X.-y. & Shih, K. 2018 Activation of persulfates using siderite as a source of ferrous ions: sulfate radical production, stoichiometric efficiency, and implications. *ACS Sustainable Chemistry & Engineering* **6**, 3624–3631.
- Ferreira, L. C., Castro-Alferez, M., Nahim-Granados, S., Polo-López, M. I. & Lucas, M. S. 2020 Inactivation of water pathogens with solar photo-activated persulfate oxidation – ScienceDirect. *The Chemical Engineering Journal* **381**, 122275.
- Guerra-Rodriguez, S., Rodriguez, E., Moreno-Andres, J. & Rodriguez-Chueca, J. 2022 Effect of the water matrix and reactor configuration on *Enterococcus* sp. inactivation by UV-A activated PMS or H<sub>2</sub>O<sub>2</sub>. *Journal of Water Process Engineering* **47**, 102740.
- Hammouda, S. B., Zhao, F., Safaei, Z., Ramasamy, D. L., Doshi, B. & Sillanpää, M. 2018 Sulfate radical-mediated degradation and mineralization of bisphenol F in neutral medium by the novel magnetic Sr<sub>2</sub>CoFeO<sub>6</sub> double perovskite oxide catalyzed peroxymonosulfate: influence of co-existing chemicals and UV irradiation. *Applied Catalysis B: Environmental* **233**, 99–111.
- Huang, W., Fei, L., Ni, Y., Lu, A., Chen, H., Liang, C. & Fei, W. 2013 Removal of trichloroethylene in groundwater with two oxidants: siderite catalyzed hydrogen peroxide and sodium persulfate. *Water Science & Technology: Water Supply* **13**, 36–43.
- Ismail, L., Ferronato, C., Fine, L., Jaber, F. & Chovelon, J. M. 2017 Elimination of sulfaclozine from water with SO<sub>4</sub><sup>•-</sup> center dot radicals: evaluation of different persulfate activation methods. *Applied Catalysis B Environmental* **201**, 573–581.
- Ji, Y., Fan, Y., Liu, K., Kong, D. & Lu, J. 2015 Thermo activated persulfate oxidation of antibiotic sulfamethoxazole and structurally related compounds. *Water Research* **87**, 1–9.
- Kholodov, V. N. & Butuzova, G. Y. 2008 Siderite formation and evolution of sedimentary iron ore deposition in the Earth's history. *Geology of Ore Deposits* **50** (4), 299–319.
- Kong, C., Liu, F., Sun, H., Zhang, Z. & Li, W. 2021a CO<sub>3</sub>O<sub>4</sub>/GO catalyst as efficient heterogeneous catalyst for degradation of wastewater containing polyacrylamide (PAM). *Water Cycle* **2**, 15–22.
- Kong, J. Y., Lu, Y., Ren, Y. R., Chen, Z. & Chen, M. H. 2021b The virus removal in UV irradiation, ozonation and chlorination. *Water Cycle* **2**, 23–31.

- Lei, Z., Sun, Z., Ma, J. & Liu, H. 2010 Influencing mechanism of bicarbonate on the catalytic ozonation of nitrobenzene in aqueous solution by ceramic honeycomb supported manganese. *Journal of Molecular Catalysis A Chemical* **322**, 26–32.
- Li, Y. H., Zhao, L., Chen, F., Jin, K. S., Fallgren, P. H. & Chen, L. 2020 Oxidation of nine petroleum hydrocarbon compounds by combined hydrogen peroxide/sodium persulfate catalyzed by siderite. *Environmental Science and Pollution Research* **27**, 25655–25663.
- Lutze, H. V., Brekenfeld, J., Naumov, S., Sonntag, C. V. & Schmidt, T. C. 2017 Degradation of perfluorinated compounds by sulfate radicals – new mechanistic aspects and economical considerations. *Water Research* **129**, 509–519.
- Ma, J., Yang, Y., Jiang, X., Xie, Z., Li, X., Chen, C. & Chen, H. 2018 Impacts of inorganic anions and natural organic matter on thermally activated persulfate oxidation of BTEX in water. *Chemosphere* **190**, 296–306.
- Mao, Y., Chen, X. W., Chen, Z., Chen, G. Q., Lu, Y., Wu, Y. H. & Hu, H. Y. 2021 Characterization of bacterial fluorescence: insight into rapid detection of bacteria in water. *Water Reuse* **11**, 621–631.
- Marjanovic, M., Giannakis, S., Grandjean, D., Alencastro, L. D. & Pulgarin, C. 2018 Effect of  $\mu\text{M}$  Fe addition, mild heat and solar UV on sulfate radical-mediated inactivation of bacteria, viruses, and micropollutant degradation in water. *Water Research* **140**, 220.
- Matilainen, A., Liikanen, R., Nystrom, M., Lindqvist, N. & Tuhkanen, T. 2004 Enhancement of the natural organic matter removal from drinking water by nanofiltration. *Environmental Technology* **25**, 283–291.
- McGuigan, K. G., Conroy, R. M., Mosler, H. J., du Preez, M., Ubomba-Jaswa, E. & Fernandez-Ibanez, P. 2012 Solar water disinfection (SODIS): a review from bench-top to roof-top. *Journal of Hazardous Materials* **235–236**, 29–46.
- Michael-Kordatou, I., Michael, C., Duan, X., He, X., Dionysiou, D. D., Mills, M. A. & Fatta-Kassinos, D. 2015 Dissolved effluent organic matter: characteristics and potential implications in wastewater treatment and reuse applications. *Water Research* **77**, 213–248.
- Pan, Y., Dong, Z., Pan, Y. & Zhang, Y. 2021 Nitriiotriacetic acid enhanced UV/FeO/H<sub>2</sub>O<sub>2</sub> process for salty wastewater treatment at neutral pH. *Water Cycle* **2**, 91–100.
- Proctor, C. R. & Hammes, F. 2015 Drinking water microbiology – from measurement to management. *Current Opinion in Biotechnology* **33**, 87–94.
- Qiao, L., Shi, Y., Cheng, Q., Liu, B. & Liu, J. 2021 The removal efficiencies and mechanism of aniline degradation by peroxydisulfate activated with magnetic Fe-Mn oxides composite. *Water Reuse* **11**, 212–223.
- Rastogi, A., Al-Abed, S. R. & Dionysiou, D. D. 2009 Sulfate radical-based ferrous-peroxymonosulfate oxidative system for PCBs degradation in aqueous and sediment systems. *Applied Catalysis B* **85**, 171–179.
- Rincon, A. G. & Pulgarin, C. 2004 Effect of pH, inorganic ions, organic matter and H<sub>2</sub>O<sub>2</sub> on *E. coli* K12 photocatalytic inactivation by TiO<sub>2</sub> – implications in solar water disinfection. *Applied Catalysis B – Environmental* **51**, 283–302.
- Rodríguez-Chueca, J., Polo-López, M., Mosteo, R., Ormad, M. P. & Fernández-Ibáñez, P. 2014 Disinfection of real and simulated urban wastewater effluents using a mild solar photo-Fenton. *Applied Catalysis B Environmental* **150–151**, 619–629.
- Rodríguez-Chueca, J., Amor, C., Fernandes, J. R., Tavares, P. B., Lucas, M. S. & Peres, J. A. 2016 Treatment of crystallized-fruit wastewater by UV-A LED photo-Fenton and coagulation-flocculation. *Chemosphere* **145**, 351–359.
- Rodríguez-Chueca, J., Silva, T., Fernandes, J. R., Lucas, M. S., Puma, G. L., Peres, J. A. & Sampaio, A. 2017 Inactivation of pathogenic microorganisms in freshwater using HSO<sub>5</sub><sup>-</sup>/UV-A LED and HSO<sub>5</sub><sup>-</sup>/Mn<sup>+</sup>/UV-A LED oxidation processes. *Water Research* **123**, 113–123.
- Rodríguez-Chueca, J., Laski, E., Garcia-Canibano, C., Martin, d. & Vidales, M. 2018 Micropollutants removal by full-scale UV-C/sulfate radical based advanced oxidation processes. *Science of the Total Environment* **630**, 1216–1225.
- Rodríguez-Chueca, J., Giannakis, S., Marjanovic, M., Kohantorabi, M. & Pulgarin, C. 2019a Solar-assisted bacterial disinfection and removal of contaminants of emerging concern by Fe<sup>2+</sup>-activated HSO<sub>5</sub><sup>-</sup> vs. S<sub>2</sub>O<sub>8</sub><sup>2-</sup> in drinking water. *Applied Catalysis B Environmental* **248**, 62–72.
- Rodríguez-Chueca, J., Guerra-Rodríguez, S., Ruez, J. M., López-Muñoz, M. & Rodríguez, E. 2019b Assessment of different iron species as activators of S<sub>2</sub>O<sub>8</sub><sup>2-</sup> and HSO<sub>5</sub><sup>-</sup> for inactivation of wild bacteria strains. *Applied Catalysis B: Environmental* **248**, 54–61.
- Sun, H., Li, G., Nie, X., Shi, H., Wong, P. K., Zhao, H. & An, T. 2014 Systematic approach to in-depth understanding of photoelectrocatalytic bacterial inactivation mechanisms by tracking the decomposed building blocks. *Environmental Science & Technology* **48**, 9412–9419.
- Tong, M., Liu, F., Dong, Q., Ma, Z. & Liu, W. 2020 Magnetic Fe<sub>3</sub>O<sub>4</sub>-deposited flower-like MoS<sub>2</sub> nanocomposites for the Fenton-like *Escherichia coli* disinfection and diclofenac degradation. *Journal of Hazardous Materials* **385**, 121604.
- Waldemer, R. A. H. H., Tratnyek, P. G., Johnson, R. L. & Nurmi, J. T. 2007 Oxidation of chlorinated ethenes by heat-activated persulfate: kinetics and products. *Environmental Science & Technology* **41** (3), 1010–1015.
- Wang, W., Wang, H., Li, G., An, T., Zhao, H. & Wong, P. K. 2019 Catalyst-free activation of persulfate by visible light for water disinfection: efficiency and mechanisms. *Water Research* **157**, 106–118.
- Wang, H. B., Wu, Y. H., Luo, L. W., Yu, T., Xu, A., Xue, S., Chen, G. Q., Ni, X. Y., Peng, L. & Chen, Z. 2021 Risks, characteristics, and control strategies of disinfection-residual-bacteria (DRB) from the perspective of microbial community structure. *Water Research* **204**, 117606.
- Wordofa, D. N., Walker, S. L. & Liu, H. 2017 Sulfate radical-induced disinfection of pathogenic *Escherichia coli* o157:h7 via iron-activated persulfate. *Environmental Science & Technology Letters* **4**, 154–160.
- World Health Organization 2016 *World Health Statistics 2016: Monitoring Health for the SDGs, Sustainable Development Goals*. World Health Organization, Geneva, Switzerland.
- Wu, Y., Bianco, A., Brigante, M., Dong, W., Sainte-Claire, P. D., Hanna, K. & Mailhot, G. 2015 Sulfate radical photogeneration using Fe-EDDS: influence of critical parameters and naturally occurring scavengers. *Environmental Science & Technology* **49**, 14343.

- Xia, D., Yan, L., Huang, G., Ran, Y. & Wong, P. K. 2017 Activation of persulfates by natural magnetic pyrrhotite for water disinfection: efficiency, mechanisms, and stability. *Water Research* **112**, 236–247.
- Xu, X. R. & Li, X. Z. 2010 Degradation of azo dye Orange G in aqueous solutions by persulfate with ferrous ion. *Separation & Purification Technology* **72**, 105–111.
- Yan, N., Liu, F., Xue, Q., Brusseau, M. L., Liu, Y. & Wang, J. 2015 Degradation of trichloroethene by siderite-catalyzed hydrogen peroxide and persulfate: investigation of reaction mechanisms and degradation products. *Chemical Engineering Journal* **274**, 61–68.
- Yin, H., Li, J., Yan, H., Cai, H., Wan, Y., Yao, G., Guo, Y. & Lai, B. 2021 Activation of peroxymonosulfate by  $\text{CuCO}_2\text{O}_4$  nano-particles towards long-lasting removal of atrazine. *Water Reuse* **11**, 542–559.
- Yu, T., Sun, H., Chen, Z., Wang, Y. H., Huo, Z. Y., Ikuno, N., Ishii, K., Jin, Y., Hu, H. Y. & Wu, Y. H. 2018 Different bacterial species and their extracellular polymeric substances (EPSs) significantly affected reverse osmosis (RO) membrane fouling potentials in wastewater reclamation. *Science of the Total Environment* **644**, 486–493.

First received 30 May 2022; accepted in revised form 21 July 2022. Available online 19 August 2022